

Electrochemistry of nanozeolite immobilized cytochrome c in aqueous and nonaqueous solutions

Kai Guo^{1,2}, Yuanyuan Hu¹, Yahong Zhang¹, Baohong Liu¹, Edmond Magner^{2}*

Department of Chemistry, Fudan University, Shanghai 200433, China and

Materials and Surface Science Institute and Department of Chemical and Environmental Sciences,
University of Limerick, Limerick, Ireland

The electrochemical properties of cytochrome c (cyt c) immobilized on multilayer nanozeolite modified electrodes have been examined in aqueous and nonaqueous solutions. Layers of **Linde** type-L zeolites were assembled on indium tin oxide (ITO) glass electrodes followed by adsorption of cyt c, primarily via electrostatic interactions, onto the modified ITO electrodes. The heme protein displayed a quasi-reversible response in aqueous solution with a redox potential of +324 mV (vs NHE), the surface coverage (Γ^*) increased linearly for the first four layers and then gave a nearly constant value of 200 pmol cm⁻². On immersion of the modified electrodes in 95% (v/v) nonaqueous solutions, the redox potential decreased significantly, a decrease that originated from changes in both the enthalpy and entropy of reduction. On re-immersion of the modified electrode in buffer, the faradic response immediately returned to its original value. These results demonstrate that nanozeolites have potential as stable supports for redox proteins and enzymes.

Introduction

The application of enzymes in biocatalysis and biosensors in aqueous systems is well established,¹ for example, nitrile hydratase is used to catalyze the hydration of acrylonitrile into acrylamide with nearly quantitative conversion of the reactants into product being obtained under mild reaction conditions.^{1a}

However, many applications require that enzymes function in nonaqueous environments. Organic synthesis, for instance, is carried out extensively in organic solvents, while many organic substrates are insoluble in water. The use of an organic phase can have a number of advantages which include: elimination of microbial contamination, reduction of interference from water-soluble compounds and enhanced thermo-stability.² The properties of proteins in organic and aqueous-organic media have been examined in detail, with a large number of studies on the rates of reaction,² protein structure³ and thermodynamics of enzyme reactions⁴ in such media. While much research has been carried out in recent years to examine the behaviour of proteins in nonaqueous media,⁵ these studies have focussed on enzymes such as lipases, with there being relatively few studies of the electrochemical properties of redox enzymes in nonaqueous media. In addition to synthetic applications, redox enzymes have the potential to be used as biosensors in nonaqueous solvents.

Redox proteins such as cytochrome c have been widely used as model systems to study biological electron transfer. Cytochrome c (horse heart) is a globular protein (12.27 kDa) consisting of 104 amino acid residues in a single polypeptide chain and a covalently attached heme group.⁶ It contains a number of lysine residues clustered around the heme edge of the protein. This high lysine content gives cytochrome c an isoelectric point (*pI*) of 9.8. The charge distribution is heterogeneous, imparting a dipole moment of 308 and 325 D for the reduced and oxidized forms, respectively, at neutral pH.⁷ The E° of cytochrome c in aqueous solution is high at 258 mV (vs. NHE), this high reduction potential arises from the π -electron-acceptor character of the thioether sulfur atom of the axially bound methionine to iron, which stabilizes the ferrous (Fe^{2+}) over the ferric (Fe^{3+}) state. This selective stabilization is further enhanced by the poor accessibility of the heme to solvent and burial of the heme within a hydrophobic pocket.⁸ The reduction of cytochrome c has been examined in a range of mixed solvents, with E° ranging from 239-247 mV in 30% acetonitrile, 40% DMSO and 50% methanol.⁹ The factors that regulate E° of cytochrome c and other heme proteins are complex and include ligand binding effects,¹⁰ degree of heme exposure to the solvent,¹¹ and the nature of the solvent medium.¹²

Insights into the correlation between $E^{\circ'}$ and structural properties of redox proteins can be obtained from the factorization of the enthalpic ($\Delta H^{\circ'}_{rc}$) and entropic ($\Delta S^{\circ'}_{rc}$) components (eq. 1). On immersion

$$E^{\circ'} = \frac{-\Delta H^{\circ'}_{rc}}{nF} + \frac{T\Delta S^{\circ'}_{rc}}{nF} \quad (1)$$

of a cytochrome c modified electrode in methanol, $E^{\circ'}$ increased by 300 mV, a change that arose from significant increases in both the enthalpy and entropy.^{4a} The change in enthalpy can be ascribed to stabilization of the ferric state by ligand binding interactions, the hydrophobic environment of the heme and the accessibility of the heme to the solvent.^{10,13} Solvent reorganization effects and changes in protein flexibility associated with reduction of cytochrome c play a major role in determining the values of the entropy change.¹⁴

However, enzymes are fragile and when used in soluble form are easily denatured and difficult to separate from the reaction mixture for reuse. Organic solvents, especially, can induce denaturation of protein. For example, myoglobin was almost fully denatured in 35-40% (v/v) methanol. In 50% methanol, the heme was extracted from the protein.^{3a} Similar results were obtained for the enzyme ervatamin C, a cysteine protease, in 50% methanol, 45% ethanol and 40% propanol.^{3b} In contrast, cytochrome c immobilized on a thiol modified electrode undergoes a reversible structural change on immersion in methanol.^{4a} Immobilization of an enzyme onto an appropriate solid support can often overcome these limitations and expand the repertoire of conditions. Different types of supports, including porous alumina,¹⁵ lipid film,¹⁶ sol-gel¹⁷ and self-assembled monolayers¹⁸ have been employed in the immobilization of enzymes. Recently, Rusling's group described the fabrication of stable films of dimyristoylphosphatidylcholine and *M.tuberculosis* catalase-peroxidase (KatG), several peroxidases, myoglobin and catalase.¹⁶ A reversible electrochemical response (Fe^{3+}/Fe^{2+}) was obtained for each protein. Direct electron transfer with hemoglobin was also achieved in electro-deposited gels. These modified electrodes were subsequently used to determine the antiviral drug rimantadine.¹⁷ Due to their chemical, mechanical and thermal stability, inorganic silica materials have attracted significant attention.

Mesoporous silicates can be used to immobilise redox proteins and enzymes in a stable and active manner.^{19(a)} Chloroperoxidase (CPO) immobilized on the mesoporous silicate, PMO PA, showed enhanced stability and activity in comparison to the enzyme in solution.^{19(b)} Direct and efficient electron transfer between a redox protein immobilised on a mesoporous silicate and the electrode is precluded as the vast majority of the protein is located within the pores of the silicate and not electrochemically addressable. Immobilisation of the protein on the surface of a support can obviate this difficulty. When cytochrome c was immobilized on NaY zeolite, direct electron transfer between the protein and the electrode was observed and the adsorbed protein could be used to electrochemically detect hydrogen peroxide.²⁰ However the loading of protein on the surface was low indicating that only protein at the surface of the electrode was electrochemically addressable. In comparison to zeolites such as NaY zeolite (where the zeolite particle have dimensions of microns), nanozeolites are significantly smaller and possess large external surface areas and high dispersibility in both aqueous and organic solutions.²¹ These properties render these materials suitable for the immobilization of enzymes and the construction of enzyme-based catalysts and sensors.²²

In this paper, a multilayer cytochrome c/nanozeolite modified ITO electrode was constructed. High loadings of electrochemically active protein were obtained with a quasi-reversible electrochemical response observed both in aqueous and nonaqueous solutions. The solvent dependence of E° ' and the rate constant of heterogeneous electron transfer are reported in a series of solvents, as well as the thermodynamics of reduction of immobilized cytochrome c.

Experimental Section

Chemicals and apparatus: Poly(diallyldimethylammonium chloride) (PDDA, MW 100,000-200,000 Da), horse heart cytochrome c, aluminum foil (0.05 mm), LUDOX SM-30 colloidal silica (30 wt.%), LiClO₄, tetraethylammonium p-toluenesulfonate (TEATS), acetonitrile, NaCl, KOH, KCl, K₂HPO₃-KH₂PO₃ were obtained from Sigma-Aldrich. Agar and ethanol were obtained from BDH and Romil, respectively. Indium tin oxide glass electrodes were supplied by the Shanghai Reagent Factory, China.

1-propanol and 1-butanol (99.9%) were obtained from Riedel-deHaen. All solutions were prepared with >18M Ω deionized water purified with an Elgastat water purification system.

XRD data were obtained on a Philips X'pert diffractometer (Ni filtered Cu $_{k\alpha}$ radiation at 40 kV and 35 mA). TEM studies were performed on a JEOL JEM-2011 electron microscope at an acceleration voltage of 200 kV. All electrochemical experiments were conducted on CHI 620A or CHI 630A potentiostats (CH Instruments).

Nanozeolite synthesis and characterization: Colloidal nano-LTL-zeolite was synthesized in a clear homogeneous solution with a molar composition of 30K $_2$ O-1Al $_2$ O $_3$ -40SiO $_2$ -1000H $_2$ O. After stirring overnight, the precursor solution was crystallized in an oven at 175°C for 24h. The colloidal nanozeolite obtained was repeatedly centrifuged (13000 rpm) and sonicated in highly pure water until the pH of the dispersion was below 8. The nanozeolite was then diluted with water to yield a 1% solution (g/g). XRD and TEM samples were prepared by drying the nanozeolite at 100 °C for 12h.

ITO electrode modification: The modified electrode was prepared by a layer-by-layer technique. ITO electrodes were cleaned with acetone, water and treated in a basic solution (NH $_4$ OH/H $_2$ O $_2$ /H $_2$ O, 1:1:5 volume ratio) to remove impurities on the electrode surface. The electrode was then alternatively immersed for 20 min in solutions of PDDA and of nanozeolite to form a homogeneous PDDA/nanozeolite multilayer. Immobilization of cyt c was achieved by immersing the multilayer modified electrode in a cyt c (0.3 mg/mL) phosphate buffer solution (PBS, 20 mM, pH 7.0) at 4 °C overnight. The electrode was then washed gently with buffer solution before use.

Electrochemical measurements of immobilized cyt c: Unless otherwise stated, all potentials reported are versus Ag/AgCl. The temperature dependence of the reduction potential was determined using a nonisothermal cell. A cell containing solvent, a multilayer cyt c modified ITO electrode and a platinum wire electrode (counter electrode) was kept under thermostatic control with a water bath and the temperature was varied from 0 to 35 °C. At the same time, a second cell containing Ag/AgCl electrode (IJ Cambria) was kept under constant temperature (25 °C). The two cells were electrical connected through a flexible 1M KCl/agar salt bridge. With this experimental configuration, ΔS°_{rc} can

be obtained from a plot of $E^{\circ'}$ versus T which is linear under the assumption of constant $\Delta S^{\circ'}_{rc}$ over the temperature range investigated. Similarly, assuming a constant value of $\Delta H^{\circ'}_{rc}$, $\Delta H^{\circ'}_{rc}$ was obtained from the slope of a plot of $E^{\circ'}/T$ versus $1/T$. Experiments at each temperature were performed at least 20 cycles. The electron-transfer rate constant (k_s) was measured from the values of ΔE_p at different scan rates using the Laviron equation.²³

Results and Discussion

Characterization of electrochemistry of cyt c/LTL in aqueous solution

The modified electrode was prepared by assembling nano-LTL-zeolite on the electrode surface using a layer-by-layer (LbL) method and then adsorbing the protein by placing the nanozeolite assembled electrode in a cyt c solution at 4°C overnight. The nano-LTL-zeolite used possesses a one-dimensional large pore system parallel to the c axis of the alumino-silicate crystal. The unit cell has hexagonal symmetry (space group P6/mmm with $a = 1.84$ nm and $c = 0.75$ nm²⁴). Transmission electron microscopy (TEM) images show the nanometer-sized cylindrical morphology (Figure 1A) and the micropore openings (Figure 1A inset). The X-ray diffraction pattern confirms the crystal structure of the zeolite (Figure 1B). Cyclic voltammograms of the cyt c modified electrode in aqueous solution showed a quasi-reversible response with an $E^{\circ'}$ of 120 ± 3 mV (Figure 2A). This increased value of $E^{\circ'}$ (by 60 mV) when compared to that in solution⁷ can be ascribed to interactions between the silanol groups on the surface of the nanozeolite and the protein.²⁵ The cathodic and anodic currents were linearly proportional to the scan rate over the range 20 to 100 mV s⁻¹ (Figure 2A inset), characteristic of a surface confined species. The response was stable with no change observed after 20 potential cycles. At scan rates of 120 mV s⁻¹ and higher, semi-infinite diffusion was observed with the peak current proportional to the square root of the scan rate. While the amount of electro-active cyt c on a self-assembled monolayer is independent of the scan rate, with the multilayer modified electrodes used here the amount of electro-active cytochrome c decreases with increasing scan rate. For an electrode modified with five layers of nanozeolite, the amount of electro-active protein at 5 V s⁻¹ was only 15% of that at a

scan rate of 0.02 V s^{-1} (Figure 2B inset). Such a significant decrease in the amount of electro-active cyt c indicates that electron transfer to and from protein layers that are distant from the electrode surface is slow; cytochrome c molecules in these layers are not electrochemically addressable at fast scan rates. As described previously,^{26, 27} electron transfer to and from cyt c in the outermost layers occurs via electron exchange between the protein layers and ultimately the electrode.

The interactions between cyt c and the nanozeolite are likely to arise from electrostatic interactions. At pH 7.5, NaY zeolite efficiently adsorbed only proteins with alkaline *pI* values and did not adsorb proteins with acidic values.²⁸ The effect of ionic strength on the adsorption of cyt c on to the nanozeolite was examined by the addition of NaCl. More than 70% of cyt c was desorbed from the nanozeolite modified electrode in the presence of 1M NaCl (Figure 3B). On re-immersion of the electrode in a solution of cyt c, 85% of the original amount was adsorbed (Figure 3C) indicating that ionic strength does not significantly alter the multilayer structure. The adsorption of cyt c onto nanozeolite modified electrodes at high ionic strength was also examined. In 1M NaCl the observed protein loading decreased by 95% (Figure 3D). These results imply that binding of cyt c is predominantly governed by electrostatic interactions.

The surface concentration of electro-active cyt c (Γ^*) in the film was obtained from the charge passed for the reduction of cyt c. The amount of electro-active protein on the surface of the film (Figure 2B) increased linearly for the first four layers, after which the response levelled off, attaining a value of 200 pmol cm^{-2} . Such a response indicates that only protein present in the layers close to the electrode surface was electro-active. Similar results were also observed for (myoglobin/SiO₂)_n or (hemoglobin/SiO₂)_n layers on pyrolytic graphite electrodes.²⁹ When only one layer of nanozeolite was present, the amount of electro-active protein on the surface was 46 pmol cm^{-2} , approximately three times the amount calculated for a monolayer of electro-active protein in buffer (assuming cyt c is a sphere 3.5 nm in diameter).⁷ This observation demonstrates that the LTL nanozeolite possesses a high binding capacity for the protein due to its large external surface area.

Electrochemical properties of cyt c/LTL in nonaqueous solutions

On placing the electrode in dry organic solvents, no faradic response was observed. However, in the presence of 5% (v/v) added water, a well defined and quasi-reversible electrochemical response was obtained in a series of solvents (at $v = 50 \text{ mV s}^{-1}$), with E° decreasing from $64 \pm 2 \text{ mV}$ (ethanol) to $-150 \pm 4 \text{ mV}$ (acetonitrile). The requirement of added water is in agreement with previous reports³⁰ which demonstrated that enzymes require a certain amount of water to function in organic solvents, with this water acting as a lubricant or plasticizer, providing the enzyme with the flexibility necessary for catalytic activity. Compared with aqueous buffer, the peak-to-peak separation values (ΔE_p) of the $\text{Fe}^{3+}/\text{Fe}^{2+}$ couple were slightly higher in all organic solvents, suggesting that the redox process is less reversible in nonaqueous environments. Similar behaviour was also obtained for the response of cyt c modified $\text{TiO}_2/\text{SnO}_2$ electrode in glycerol.^{30a} The E° value of cyt c³¹ is sensitive to the conformation of the protein and the properties of the solvent medium. The decrease in E° can arise from a number of changes. These include structural changes to the protein and alterations in the interactions between the protein and the nanozeolite in nonaqueous solutions. Small structural changes could alter the degree of accessibility of the heme to the solvent. An increase in the degree of accessibility of the heme on binding to silicate surfaces has been proposed to account for slightly higher rates of reaction with the dye ABTS.³² In addition, the electrostatic interactions between the protein and the nanozeolite would be expected to be stronger in nonaqueous environments; such changes would preferentially stabilize the Fe^{3+} form.

On re-immersion of the electrodes in buffer, the faradic response returned to its original value immediately in all solvents (Figure 4). While there is significant discussion as to whether or not the heme group remains within the heme binding pocket when myoglobin and horseradish peroxidase is immobilized on electrode surfaces.³² The observed increase in E° indicates that the heme is bound to the protein (E° of hemin is -350 mV^{31}). In addition, the heme group in cyt c is covalently attached to the polypeptide chain and is not easily removed,³³ with the procedure for the removal of heme involving

harsh conditions. Raman spectroscopic data of cytochrome c adsorbed on mesoporous silicates³⁴ and on TiO₂^{30(a)} surfaces in a range of nonaqueous solvents, demonstrating that the heme environment of the protein is unchanged.

No electrochemical response was observed in tetrahydrofuran and ethyl acetate. The faradaic response of adsorbed cyt c in ethanol, 1-propanol, 1-butanol and acetonitrile was stable with no changes evident after 30 scans. A quasi-reversible faradic response with an E° of -57 ± 5 mV (vs.Ag/AgCl) was observed in methanol. This response decreased dramatically after storage for 2 minutes. This response contrasts that observed with cyt c on a self-assembled monolayer (SAM) in methanol^{3a} where an increase in E° of 300 mV was observed. On re-immersion in aqueous buffer solution, the original faradaic response was restored over a period of 120 min. The rapid return of the faradaic response to its original value in buffer indicates that adsorption of cytochrome c onto the nanozeolite likely occurs in a manner which restricts the conformational mobility of the protein in comparison to that of the protein adsorbed on a thiol modified electrode. Recent studies with zeolite molecular sieves have shown that these materials can be used to increase the activity and enhance the stability of adsorbed proteins in organic solvents.³⁵

For an electrode modified with 5 layers of nanozeolites, the electron-transfer rate constant (k_s)²³ was 10.9 ± 2.5 s⁻¹ in aqueous buffer ($\alpha=0.5$) (Figure 5A). Values of 11.1 ± 1.4 s⁻¹ and 9.8 ± 1.2 s⁻¹ were obtained for three and one layers, respectively, indicating that the rate constant was homogeneous and independent of the number of layers. These values are in good agreement with the values previously observed (1.0-18 s⁻¹) at tin oxide electrodes,³⁴ but significantly lower than that observed for layers of cytochrome c adsorbed within polyaniline sulfonate assembled on a gold electrode (75 s⁻¹).²⁶ This may be ascribed to the thickness of the nanozeolite films which are more than 400 nm for an electrode with 5 layers³⁷ while the enzyme/polyaniline sulfonate layers are less than 100 nm.³⁸ This increase in the distance between the protein and the electrode could account for the lower value of k_s . The value of k_s decreased to 4.6 ± 1.4 s⁻¹ in acetonitrile, 3.7 ± 0.9 s⁻¹ in ethanol, 2.9 ± 0.4 s⁻¹ in 1-propanol and 2.1 ± 0.3 s⁻¹ in 1-butanol. A decrease in k_s was also observed for cyt c dissolved in 40% DMSO with k_s decreasing

by a factor of 7 from $3.54 \times 10^{-3} \text{ cm s}^{-1}$ in buffer to $0.44 \times 10^{-3} \text{ cm s}^{-1}$ in mixed solvent.³⁸ These data indicate that the effect of the organic solvent on k_s is complex, with the effect varying from solvent to solvent.

Thermodynamic investigation of cyt c/LTL electrode

The effect of temperature on reduction potential in both aqueous and nonaqueous solutions was studied (Figure 6A). In all solvents, a linear decrease in $E^{\circ'}$ was obtained with temperature over the range 0 to 35 °C resulting in decreases $\Delta H^{\circ'}_{rc}$ and $\Delta S^{\circ'}_{rc}$ for the reduction of cyt c. The value of $\Delta S^{\circ'}_{rc}$ in phosphate buffer solution was $-94.5 \text{ J K}^{-1} \text{ mol}^{-1}$, a decrease when compared to that measured in solution ($-44 \text{ J K}^{-1} \text{ mol}^{-1}$).¹⁰ The reduction entropy of redox proteins is considered to be due to solvent induced reorganization effects, variation of solvent dielectric about the metal redox centers and the influence of ligation.¹⁴ **The value obtained here indicates that significant structural and/or solvation related entropy changes occurred upon reduction of cyt c, rendering oxidation of Fe^{2+} even more entropically favorable.** It is not feasible to identify which specific factors cause this entropy change. Oxidation of the protein introduces an additional positive charge to the protein and may increase the degree of binding between the protein and support, rendering the protein less conformationally flexible.

The value of $\Delta H^{\circ'}_{rc}$ in aqueous solution obtained from a plot of $E^{\circ'}/T$ versus $1/T$ (Figure 6B) decreased significantly to $-60.3 \text{ kJ mol}^{-1}$ (solution value of $-35.6 \text{ kJ mol}^{-1}$),¹⁰ favoring reduction of immobilized cytochrome c. Despite the substantial decrease in $\Delta S^{\circ'}_{rc}$, the change in $\Delta E^{\circ'}$ is primarily determined by $\Delta H^{\circ'}_{rc}$ (Table 1). The enthalpy of reduction is a function of a range of effects including the nature of the axial ligand(s), the net charge of both the heme and the protein, the extent of the hydrogen bonding network and the degree of solvent exposure.¹³

The thermodynamic parameters for the reduction of cyt c adsorbed on nanozeolite modified electrodes in organic solvents are reported in Table 1. The presence of organic solvent in the solution changes $\Delta H^{\circ'}_{rc}$ and $\Delta S^{\circ'}_{rc}$ with respect to aqueous buffer with the overall effects of decreasing $E^{\circ'}$. The enthalpy and entropy changes are solvent dependent. The $\Delta S^{\circ'}_{rc}$ value for cyt c in 1-propanol is slightly **lower**

than in aqueous buffer, while ΔH°_{rc} is much higher than the value in PBS. These enthalpic and entropic contributions to E° in 1-propanol are +384 and -296 mV, relative to the values of +618 and -295 mV, respectively in buffer. This clearly indicates that the decrease in E° (+89 mV vs.NHE) in 1-propanol is mainly enthalpic in origin and stems from enhanced stabilization of the ferriheme (Fe^{3+}). On the other hand, in 1-butanol or acetonitrile, ΔS°_{rc} becomes the dominant factor, -535 mV in 1-butanol and -697 mV in acetonitrile. In entropic terms as seen previously, replacement of water by 1-butanol or acetonitrile would be expected to favor reduction because the ferric form possesses an extra positive charge in a more hydrophobic environment,¹⁴ but this is not the case here. In ethanol, both ΔH°_{rc} and ΔS°_{rc} increased in comparison to aqueous buffer with the overall effect of decreasing E° , with enthalpy and entropy contributions to ΔE° of -144 and 88 mV, respectively (Table 2). **No correlations between properties such as solvent dielectric constant and E° , ΔH° or ΔS° of cyt c at nanozeolites were observed (Figure S1, 2 and 3). This observation is in agreement with previous reports on cytochrome c⁹ and microperoxidase-11,⁴⁰ where the redox potential similarly did not show any correlation with solvent properties.**

The response of (cyt c/nano-LTL-zeolite)_n ITO to hydrogen peroxide was evaluated in acetonitrile. Using a 5-layer nanozeolites modified ITO electrode, a stable response with sufficiently high sensitivity was observed in 95% (v/v) acetonitrile with a linear response over the range of 25-660 μ M. The limit of detection in acetonitrile was 500 nM which is **similar to that observed for cyt c adsorbed on NaY zeolite** (20) magnitude higher than in buffer.³⁰ This response indicates that nanozeolites provide a stable means of immobilization redox proteins.

Conclusions

The electrochemical properties of cyt c immobilised on nanozeolites were evaluated in aqueous buffer and organic solvents. Nano-LTL-zeolite was used as an enzyme carrier to construct (cyt c/nano-LTL-zeolite)_n ITO electrodes by a layer-by-layer (LbL) technique. Adsorbed cyt c displayed a quasi-reversible faradic response in aqueous solution. Immobilization via electrostatic interactions on ITO resulted in a

increase in E° in comparison to cytochrome c in solution. The level of surface coverage (Γ^*) indicated that multi-layer protein adsorption occurred on ITO. Replacement of water by organic solvents resulted in a decrease in the E° of cyt c, which originated from changes in both the enthalpy and entropy of reduction. Upon re-immersion in buffer, the faradic responses returned to the original values which showed the protection of enzyme from organic solvents. These results signify that nanozeolites are suitable carriers for the immobilization of redox proteins.

Acknowledgement

This work is supported by China Ireland programme, Science Foundation Ireland, the Programme for Research in Third Level Institutions (INSPIRE) and NSFC 20925517. TEM images were obtained by Dr. Calum Dickinson.

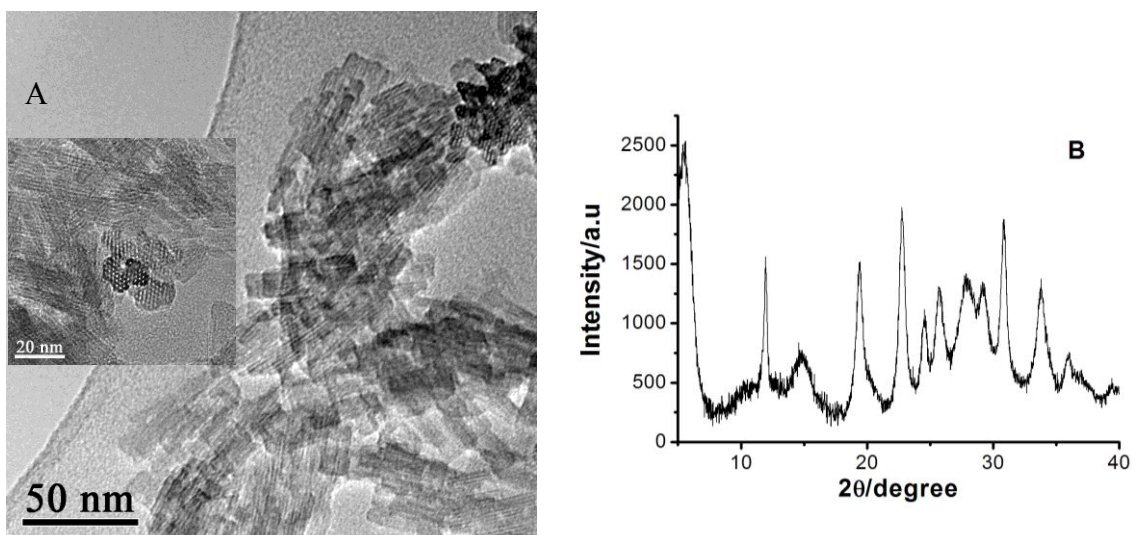


Figure 1. A) TEM image of LTL nanozeolite; B) XRD pattern of LTL nanozeolite. The bars in TEM images are 50 nm and 20 nm (inset).

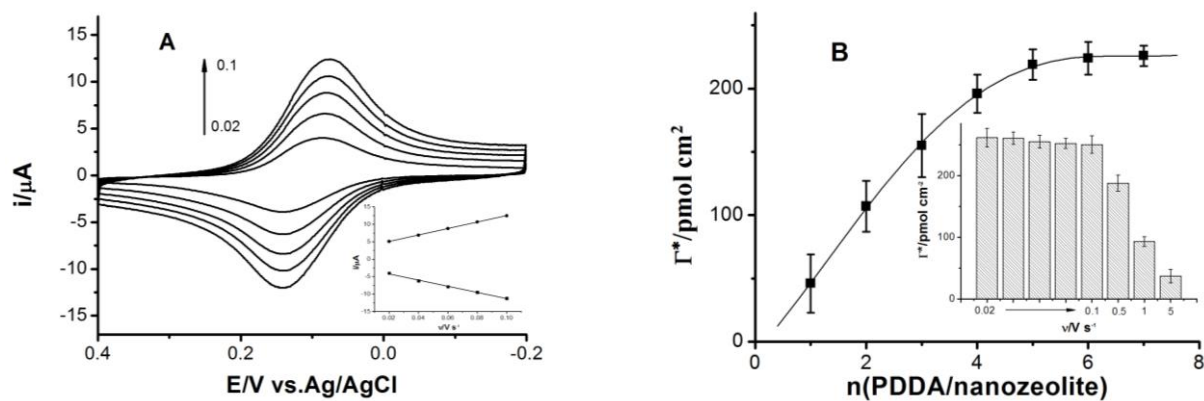


Figure 2. A) Cyclic voltammograms of cyt c/nanozeolite (5 layers) in 20 mM PBS at pH 7.0 over a range of scan rates (0.02 to 0.1 V s^{-1}). Inset: plots of anodic (\bullet) and cathodic (\square) peak currents vs scan rate. B) Surface coverage of electrochemically addressable cyt c immobilized in 1-7 layers of nano-LTL-zeolite; n = number of layers of PDDA/nano-LTL-zeolite, $v = 0.05 \text{ V s}^{-1}$. Inset: Electrochemically addressable surface coverage of adsorbed cyt c (5 layers) at different scan rates.

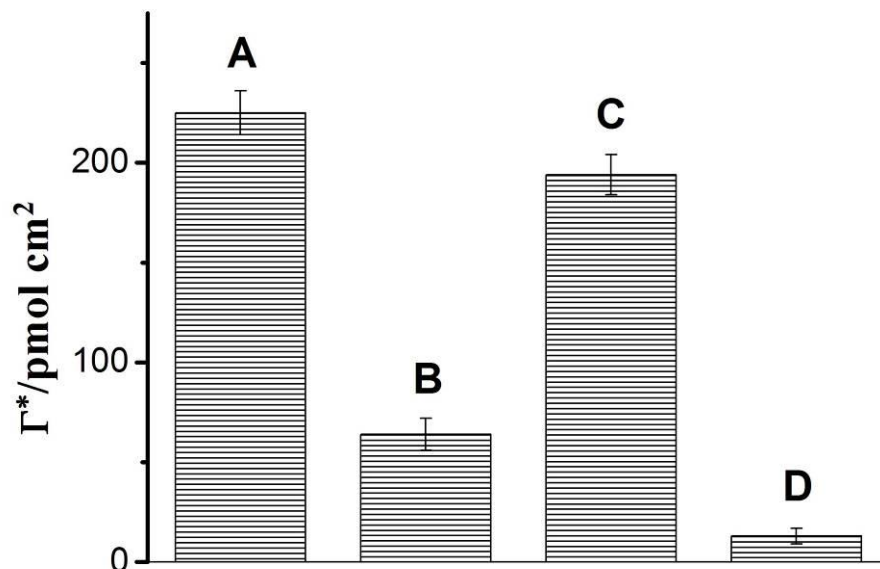


Figure 3. Surface coverage of the electro-active cyt c immobilized on A) nanozeolite (5 layers) modified ITO electrode, B) after storage in 1M NaCl for 60 min, C) after re-immersion in 0.3 mg mL⁻¹ cyt c, D) nanozeolite (5 layers) modification with 1M NaCl in cyt c solution, $v = 0.05 \text{ V s}^{-1}$.

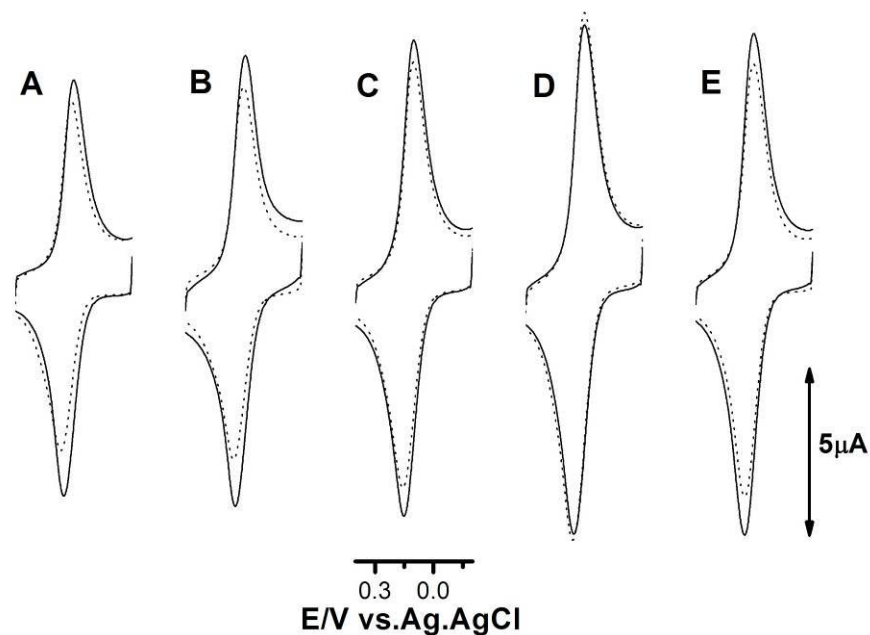


Figure 4. Sample CVs of adsorbed cyt c in aqueous buffer (—) before and after (.....) storage in organic solvents for 60 min: A) methanol, B) ethanol, C) 1-propanol, D) 1-butanol and E) acetonitrile. Conditions: scan rate 0.05 V s^{-1} at 20°C , 20 mM phosphate buffer, pH 7.0.

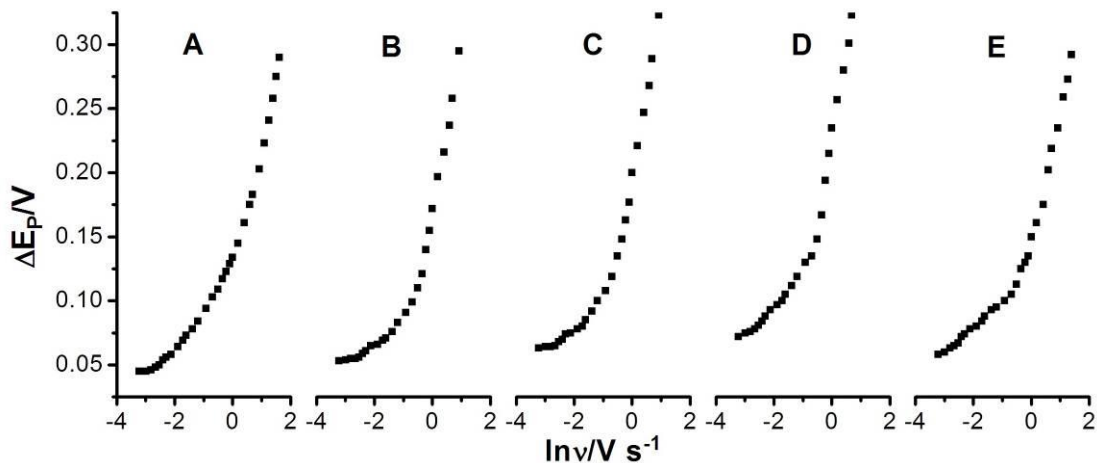


Figure 5. Relationship between the peak-to-peak separation and the scan rate of cyt c/nanozeolite (5layers) in different solvents: A) PBS ($10.9 \pm 2.5 \text{ s}^{-1}$), B) ethanol ($3.7 \pm 0.9 \text{ s}^{-1}$), C) 1-propanol ($2.9 \pm 0.4 \text{ s}^{-1}$), D) 1-butanol ($2.1 \pm 0.3 \text{ s}^{-1}$), E) acetonitrile ($4.6 \pm 1.4 \text{ s}^{-1}$).

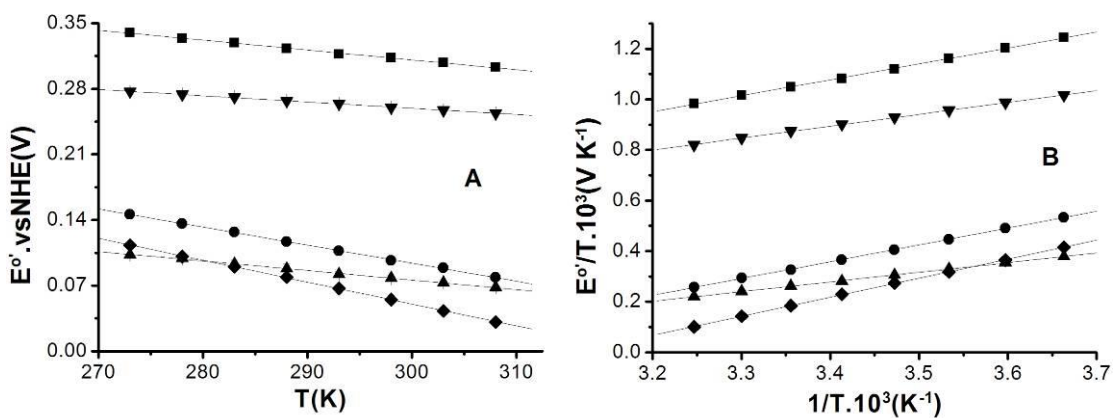


Figure 6. Plots of A) E° vs temperature for cyt c absorbed onto multilayer nanozeolite in PBS (■), ethanol (▼), 1-propanol (●), 1-butanol (▲) and acetonitrile (◆) and B) E°/T vs $1/T$ of the data in A. Data points represent the mean E° at each temperature ± 1 standard deviation ($n=3$), $v = 0.05 \text{ V s}^{-1}$.

Table 1. Thermodynamic data for the reduction of cyt c adsorbed on multilayer nanozeolite in different solvents

Solvent	$E^{\circ'}$ (mV) ^a	ΔE_p (mV) ^b	$\Delta H^{\circ'}$ (kJ.mol ⁻¹)	$\Delta S^{\circ'}$ (J K ⁻¹ .mol ⁻¹)	$-\Delta H^{\circ'}/nF$ (mV)	$T\Delta S^{\circ'}/nF$ (mV)
PBS	324±3	45±2	-60.3	-94.5	618	-295
EtOH	268±2	54±5	-45.4	-67.5	474	-207
1-Prop	89±2	64±3	-36.7	-96.5	384	-296
1-But	124±2	75±2	-63.7	-173.3	660	-535
ACN	54±4	60±3	-72.4	-225.8	750	-697

^a with respect to NHE at 20 °C. ^b Values for ΔE_p are based on three individual determinations at scan rates of 0.05 V s⁻¹.

Table 2. Changes in thermodynamic parameters for reduction of nanozeolite adsorbed cyt c in different solutions

Species	$\Delta E^{\circ'}$ (mV)	$\Delta\Delta H^{\circ'}/nF$ (mV)	$T\Delta\Delta S^{\circ'}/nF$ (mV)
(cyt c/LTL)-(cyt c _(N))	60	222	-162
(cyt c/LTL _{EtOH})-(cyt c/LTL _{PBS})	-56	-144	88
(cyt c/LTL _{1-Prop})-(cyt c/LTL _{PBS})	-235	-234	-1
(cyt c/LTL _{1-But})-(cyt c/LTL _{PBS})	-100	42	-142
(cyt c/LTL _{ACN})-(cyt c/LTL _{PBS})	-270	132	-402

Reference:

- (1) (a) Nagasawa, T.; Yamada, H. *Pure Appl. Chem.* **1990**, *62*, 1441. (b) Katz, E.; Willner, I. *Angew. Chem. Int. Ed.* **2004**, *43*, 6042
- (2) Das, P. K.; Caaveiro, J. M. M.; Luque, S.; Klibanov, A. M. *J. Am. Chem. Soc.* **2002**, *124*, 782.
- (3) (a) Babu, K. R.; Douglas, D. J. *Biochemistry* **2000**, *39*, 14702. (b) Abbyad, P.; Shi, X. H.; Childs, W.; McAnaney, T. B.; Cohen, B. E.; Boxer, S. G. *J. Phys. Chem. B* **2007**, *111*, 8269.
- (4) (a) Crilly, S.; Magner, E. *Chem. Comm.* **2009**, 535. (b) Borsari, M.; Bellei, M.; Tavagnacco, C.; Peressini, S.; Millo, D.; Costa, G. *Inorg. Chim. Acta.* **2003**, *349*, 182.
- (5) Schmid, A.; Dordick, J.S.; Hauer, B.; Kiener, A.; Wubbolts, M.; Witholt, B. *Nature*, 2001, **409**, 258.
- (6) Scott, R. A.; Mauk, A. G. *Cytochrome c: A Multidisciplinary Approach*; University Science Books: Sausalito, California, 1996.
- (7) Hildebrandt, P.; Heimburg, T.; Marsh, D.; Powell, G. L. *Biochemistry* **1990**, *29*, 1661.
- (8) (a) Schejter, A.; Plotkin, B.; Vig, I. *FEBS Lett.* **1991**, *280*, 199. (b) Tezcan, F. A.; Winkler, J. R.; Gray, H. B. *J. Am. Chem. Soc.* **1998**, *120*, 13383.
- (9) O'Reilly, N. J.; Magner, E. *Langmuir* **2005**, *21*, 1009.
- (10) Battistuzzi, G.; Borsari, M.; Cowan, J. A.; Ranieri, A.; Sola, M. *J. Am. Chem. Soc.* **2002**, *124*, 5315.
- (11) Stellwagen, E. *Nature* **1978**, *275*, 73.
- (12) (a) O'Donoghue, D.; Magner, E. *Chem. Comm.* **2003**, 438. (b) O'Donoghue, D.; Magner, E. *Electrochim. Acta.* **2007**, *53*, 1134.

- (13) Battistuzzi, G.; Borsari, M.; Loschi, L.; Righi, F.; Sola, M. *J. Am. Chem. Soc.* **1999**, *121*, 501.
- (14) Bertrand, P.; Mbarki, O.; Asso, M.; Blanchaed, L.; Guerlsquin, F.; Tegoni, M. *Biochemistry* **1995**, *34*, 11071.
- (15) Ikeda, O.; Ohtani, M.; Yamaguchi, T.; Komura, A. *Electrochim Acta* **1998**, *43*, 833.
- (16) Zhang, Z.; Chouchane, S.; Magliozzo, R. S.; Rusling, J. F. *Anal. Chem.* **2002**, *74*, 163.
- (17) Rozhanchuk, T.; Tananaiko, O.; Mazurenko, I.; Etienne, M.; Walcarius, A.; Zaitsev, V. *J. Electroanal. Chem.* **2009**, *625*, 33.
- (18) Chen, X.; Ferrigno, R.; Yang, J.; Whitesides, G. M. *Langmuir* **2002**, *18*, 7009.
- (19) Hudson, S.; Cooney, J.; Hodnett, B. K.; Magner, E. *Chem. Mater.* **2007**, *19*, 2049.
- (20) Dai, Z. H.; Liu, S. Q.; Ju, H. X. *Electrochimica Acta* **2004**, *49*, 2139.
- (21) Shan, W.; Zhang, Y. H.; Yang, W. L.; Ke, C.; Gao, Z.; Ye, Y. E.; Tang, Y. *Microporous Mesoporous Mater.* **2004**, *69*, 35.
- (22) (a) Yu, T.; Zhang, Y.H.; You, C. P.; Zhuang, J. H.; Wang, B.; Liu, B. H.; Kang, Y. J.; Tang, Y. *Chem. Eur. J.* **2006**, *12*, 1137. (b) Ji, J.; Zhang, Y. H.; Zhou, X. Q.; Kong, J. L.; Tang, Y.; Liu, B. H. *Anal. Chem.* **2008**, *80*, 2457.
- (23) E. Laviron, *J. Electroanal. Chem.* **1979**, *101*, 19.
- (24) Meng, X.; Zhang, Y.; Meng, C.; Pang, W. *Proceedings of the 9th International Zeolite Conference*, Montreal, 1992.
- (25) Kriel, L. W.; Jimenez, V. L.; Balkus, K. J. *J. Mol. Catal. B: Enzym.* **2000**, *10*, 453.
- (26) Beissenhirtz, M. K.; Scheller, F. W.; Stoklein, W. F. M.; Kurth, D. G. Mohwald, H.; Lisdat, F. *Angew. Chem. Int. Ed.* **2004**, *43*, 4357.

- (27) He, P. L.; Hu, N. F.; Rusling, J. F. *Langmuir* **2004**, *20*, 722.
- (28) Masayoshi, M.; Yoshimichi, K.; Taichi, Y.; Yoshiyuki, M.; Fujio, M.; Kengo, S.. *Chem. Eur. J.* **2001**, *7*, 1555.
- (29) Xie, Y.; Liu, H. Y.; Hu, N. F. *Bioelectrochemistry* **2007**, *70*, 311.
- (30) (a) Grealis, C.; Magner, E. *Langmuir* **2003**, *19*, 1282. (b) Konash, A.; Magner, E. *Biosens. Bioelectron.* **2006**, *22*, 116.
- (31) King, B. C.; Hawkrigde, F. M.; Hoffman, B. M. *J. Am. Chem. Soc.* **1992**, *114*, 10603.
- (32) Magner, E.; McLendon, G. *J. Phys. Chem.*, **1989**, *93*, 7130.
- (33) Brusowa, Z.; Gorton, L.; Magner, E. *Langmuir*, **2006**, *22*, 11453.
- (34) (a) Deere, J.; Serantoni, M.; Edler, K. J.; Hodnett, B. K.; Wall, J. G.; Magner, E. *Langmuir* **2004**, *20*, 532, (b) Deere, J.; Magner, E.; Wall, J.G.; Hodnett, B.K. *Biotech. Prog.*, **2003**, *19*, 1238.
- (35) Gonqalves, A. P. V.; Lopes, J. M.; Lemos, F.; Ribeiro, F. R.; Prazeres, D. M. F.; Cabral, J. M. S.; Aires-Barros, M. R. *J. Mol. Catal. B: Enzym.* **1996**, *1*, 53.
- (36) Willit, J. L.; Bowden, E. F. *J. Phys. Chem.* **1990**, *94*, 8241.
- (36) Zhang, H.; Chen, F.; Shan, W.; Zhuang, J. H.; Dong, A. G.; Cai, W. B.; Tang, Y. *Microporous Mesoporous Mater.* **2003**, *65*, 277.
- (37) Shutava, T. G.; Kommireddy, D. S.; Lvov, Y. M. *J. Am. Chem. Soc.* **2006**, *128*, 9926.
- (38) Sivakolundu, S. G.; Mabrouk, P. A. *J. Am. Chem. Soc.* **2000**, *122*, 1513.
- (39) Battistuzzi, G.; Borsari, M.; Rossi, G.; Sola, M. *Inorg. Chim. Acta.* **1998**, *272*, 168.
- (40) O'Donoghue, D., Magner, E. *Electrochim. Acta*, **2007**, **53**, 1134-1139.

Electrochemistry of nanozeolite immobilized
cytochrome c in aqueous and nonaqueous solutions

Kai Guo^{1,2}, Yuanyuan Hu¹, Yahong Zhang¹, Baohong Liu¹, Edmond.Magner^{2}*

Department of Chemistry, Fudan University, Shanghai 200433, China and

Materials and Surface Science Institute and Department of Chemical and Environmental Sciences,
University of Limerick, Limerick, Ireland

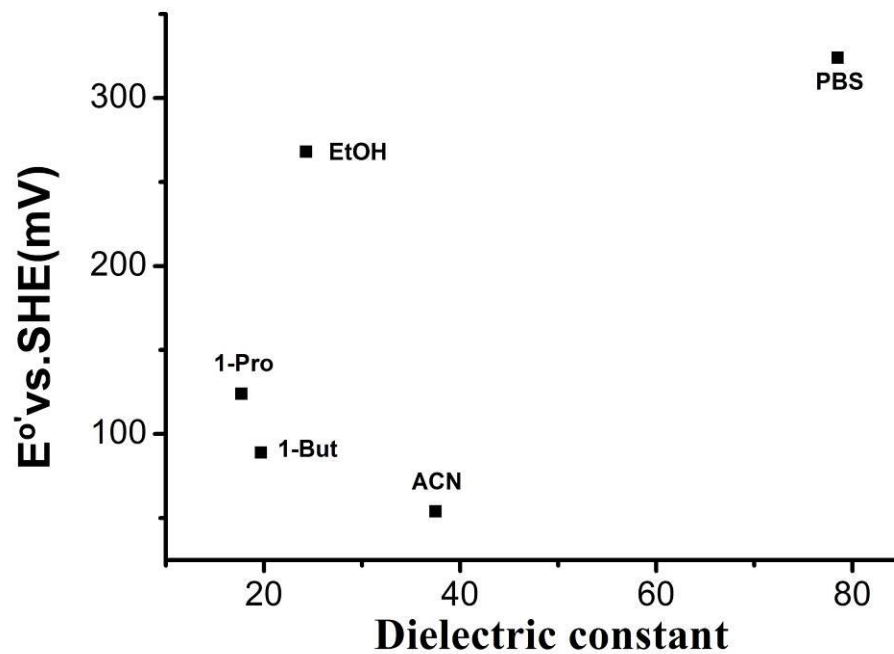


Figure S1. Plot of E° vs. dielectric constant at 293 K for each solvent.

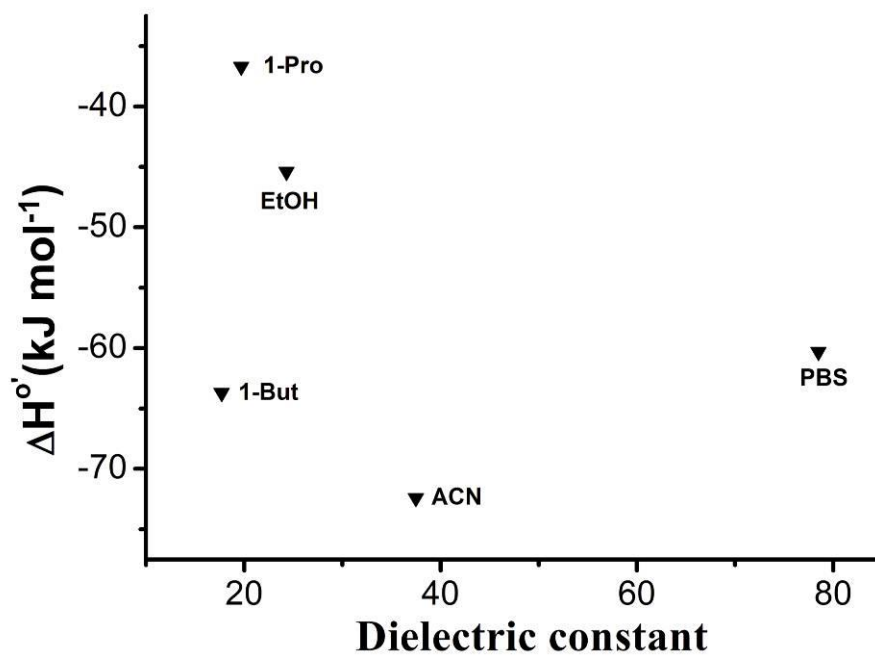


Figure S2. Plot of ΔH° vs. dielectric constant at 293 K for each solvent.

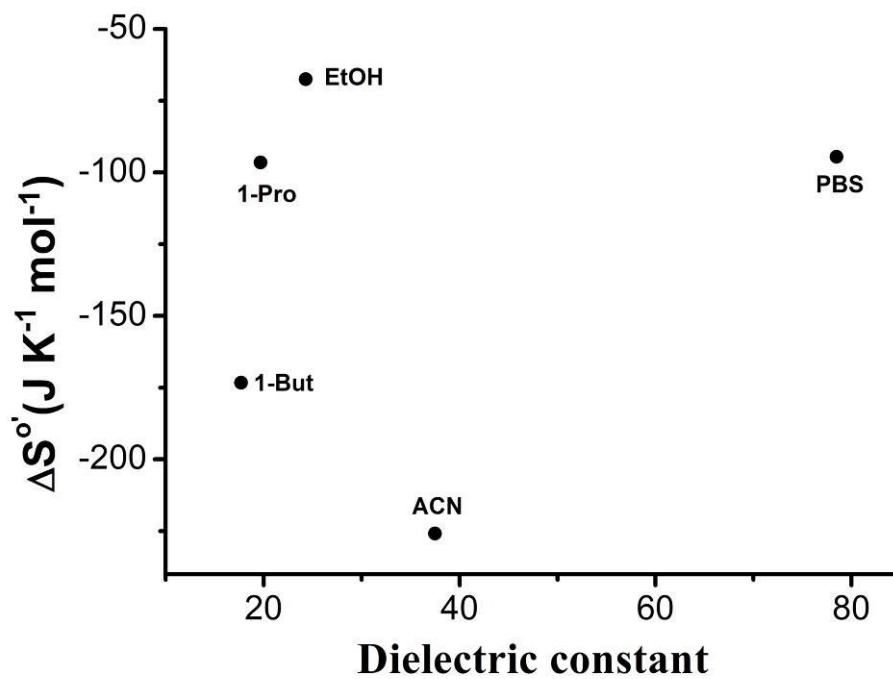


Figure S3. Plot of ΔS° vs. dielectric constant at 293 K for each solvent.